

TURBULENT HEAT TRANSPORT ACROSS AN ENCLOSURE CONTAINING A POROUS LAYER OF VARIABLE THICKNESS

Viviani T. Magro
Daniel Rezende Graminho
Marcelo J.S. De-Lemos *

Departamento de Energia – IEME
Instituto Tecnológico de Aeronáutica – ITA
12228-900 - São José dos Campos - SP – Brazil

* Corresponding author. E-mail: delemos@mec.ita.br

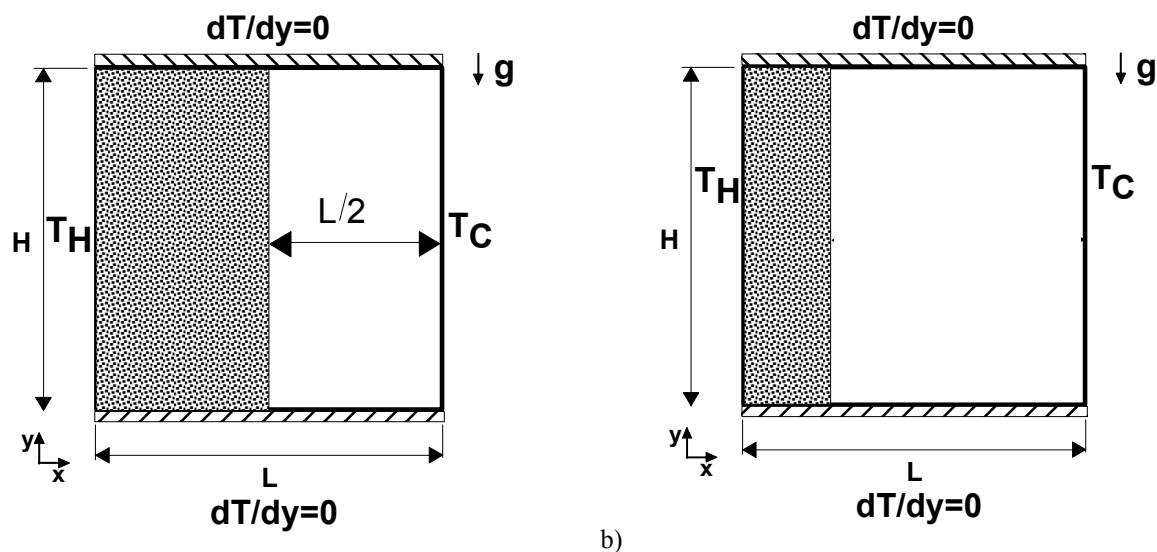
Abstract. This work presents numerical solutions for flow and heat transfer in square cavities partially obstructed with porous material. The microscopic flow and energy equations are integrated in a representative elementary volume in order to obtain a set of equations valid in both the clear flow region and in the porous matrix. A unique set of equations is discretized with the control volume method and solved with the SIMPLE algorithm. Enhancement of convective currents within the porous substrate is detected as the Rayleigh number Ra increases. Thin boundary layers along the cavity vertical walls and stratification of the thermal field are observed for $Ra > 10^9$. Results further show that for high values of Ra the thickness of the porous layer becomes of a lesser importance.

Keywords. Natural Convection, Turbulence Model, Porous Media, Heat Transfer

1. Introduction

The study of natural convection in composite enclosures having layers of distinct materials, have several applications of great engineering relevance. Insulating systems in engineering equipment often use layers of porous material with the aim of controlling heat transfer rates across heated surfaces. In addition, advanced nuclear reactor systems consisting of a reactor core embedded in a large coolant pool are considered to be inherently safe since the heat generated in the event of an accident is passively removed the action of gravity. In many of these systems, materials and components can be modeled as a porous structure in an enclosure subjected to natural convection currents.

When treating turbulent flow in porous media, recent works in the literature propose a macroscopic treatment of the properties of interest, integrating these quantities in a representative elementary volume so that macroscopic equations for the flow arise [Anthohe & Lage (1997), Pedras & de Lemos (2001)]. With respect to cavity flows in clear and in porous media, subjected to a temperature gradient across the layer, the literature is vast and a great number of solutions can be found, so much for clear cavities de Vahl Davis (1983) as for porous enclosures Charrier-Mojtabi (1997). Also for this geometry, the work of Braga & de Lemos (2002a) presents results for laminar convection in square cavities heated on the sides. Later, Braga & de Lemos (2002b) extended their results to horizontal annuli. Turbulent flow in eccentric and concentric annuli was also investigated Braga & de Lemos (2002c). Also, a study on natural convection in cavities completely filled with porous material was presented in Braga & de Lemos (2002d). In this last work, the two geometries previously analyzed, namely square and annular region, were considered. More recently, Braga & de Lemos (2002e) presented results for laminar and turbulent flow in square cavity for clear and porous media. The modeling of the turbulent natural convection in porous enclosures is fully documented in de Lemos & Braga (2003). The turbulence model employed is the standard $k-\epsilon$ turbulence model with wall function.



a) b)
Figure 1 Cases analyzed a) Cavity with 50% porous material; b) Cavity with 25% at porous material.

In all the results mentioned above, the considered cavity was either totally clear or totally filled with a porous substrate. In this work, the considered problem is shown schematically in Figure 1. Here, the situation considered treats two-dimensional flow of an incompressible fluid in a square cavity of height H and width L , partially filled with porous material with different thicknesses. Further, for the cavity of the illustration one considers constant temperatures on the left face, T_H , and on the right, T_C , being $T_H > T_C$. The other two walls are maintained insulated.

In Magro & de Lemos (2002a) laminar flow and heat transfer in the cavity of the Figure 1 were investigated. In that work, the effect of the number of Rayleigh and the treatment of the interface, located at $x=L/2$, were the objective of the analysis. There, the interface treatment used was the one proposed in Ochoa-Tapia & Whitaker (1995). Later, in Magro & de Lemos (2002b) the previous investigation was complemented, taken then into account the effects of porosity and permeability of the porous region. In both works, the analysis was made for flow in laminar regime. Recently, Magro & de Lemos (2002b) and de Lemos & Magro (2003) considered turbulent flow in a cavity having 50% of its volume occupied by a porous material.

The objective of this contribution is to extend former results in cavity considering now turbulent flow in the cavities of Figure 1, including now simulation of heat transfer across the enclosure when only 25% of the total space is occupied by the permeable medium. Nusselt numbers for the both cases shown in the figure are compared.

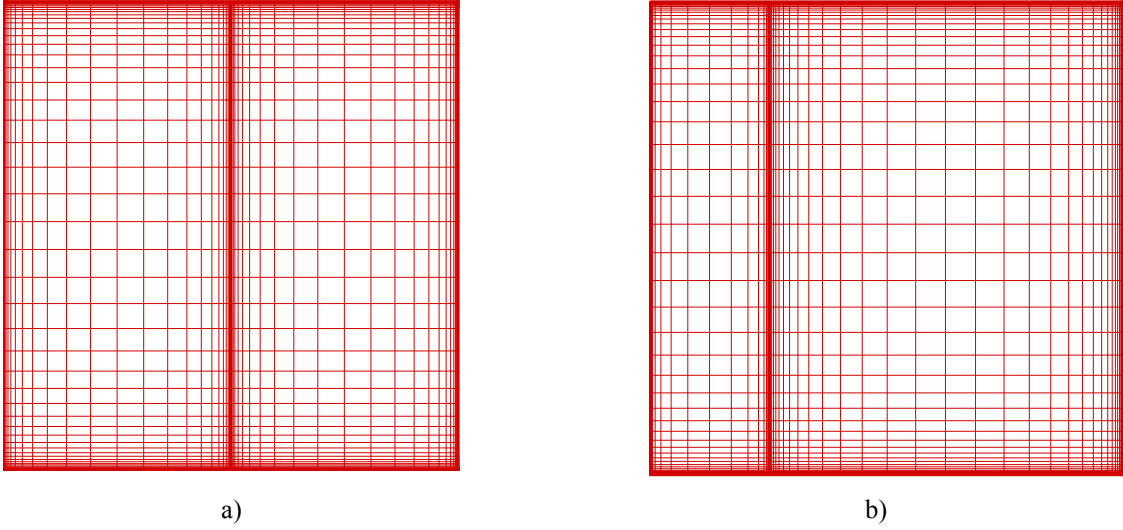


Figure 2 Computational grids; a) Grid for case a) in Figure 1, b) Grid for case b) in Figure 2.

2. Mathematical Model

The mathematical model here employed has its origin in the works of Pedras & de Lemos (2001) for the hydrodynamic field and e Rocamora & de Lemos (2000) for the thermal field. The consideration of buoyancy forces was taken in the works of Braga & de Lemos (2002a-e) and the implementation of the jump condition at the interface was considered in Silva & de Lemos (2002) based on the theory proposed in Ochoa-Tapia & Whitaker (1995). Therefore, these equations will be here just reproduced and details about their derivations can be obtained in the mentioned works. These equations are:

2.1 Macroscopic continuity equation:

$$\nabla \cdot \bar{\mathbf{u}}_D = 0 \quad (1)$$

where, $\bar{\mathbf{u}}_D$ is the average surface velocity ('seepage' or Darcy velocity). The equation (1) represents the macroscopic continuity equation for an incompressible fluid.

2.2 Macroscopic momentum equation:

$$\left[\nabla \cdot \left(\rho \frac{\bar{\mathbf{u}}_D \bar{\mathbf{u}}_D}{\phi} \right) \right] = -\nabla(\phi \langle \bar{p} \rangle^i) + \mu \nabla^2 \bar{\mathbf{u}}_D + \nabla \cdot (-\rho \phi \langle \overline{\mathbf{u}' \mathbf{u}'} \rangle^i) - \rho \beta_\phi \mathbf{g} \phi (\langle \bar{T} \rangle^i - T_{ref}) - \left[\frac{\mu \phi}{K} \bar{\mathbf{u}}_D + \frac{c_F \phi \rho |\bar{\mathbf{u}}_D| \bar{\mathbf{u}}_D}{\sqrt{K}} \right] \quad (2)$$

where the last two terms in equation (2), represent the Darcy-Forchheimer contribution. The symbol K is the porous medium permeability, c_F is the form drag coefficient (Forchheimer coefficient), $\langle \bar{p} \rangle^i$ is the intrinsic average pressure of

the fluid, ρ is the fluid density, μ represents the fluid viscosity and ϕ is the porosity of the porous medium. The macroscopic Reynolds stress $-\rho\phi\langle\overline{\mathbf{u}'\mathbf{u}'}\rangle^i$ is given as,

$$-\rho\phi\langle\overline{\mathbf{u}'\mathbf{u}'}\rangle^i = \mu_{t_\phi} 2\langle\overline{\mathbf{D}}\rangle^v - \frac{2}{3}\phi\rho\langle k\rangle^i \mathbf{I} \quad (3)$$

where

$$\langle\overline{\mathbf{D}}\rangle^v = \frac{1}{2}\left[\nabla(\phi\langle\overline{\mathbf{u}}\rangle^i) + [\nabla(\phi\langle\overline{\mathbf{u}}\rangle^i)]^T\right] \quad (4)$$

is the macroscopic deformation tensor, $\langle k\rangle^i = \langle\overline{\mathbf{u}'\mathbf{u}'}\rangle^i/2$ is the intrinsic turbulent kinetic energy, k , and μ_{t_ϕ} , is the turbulent viscosity which is modeled in Pedras & de Lemos (2001) similarly to the case of clear flow, in the form,

$$\mu_{t_\phi} = \rho c_\mu \frac{\langle k\rangle^{i2}}{\langle\epsilon\rangle^i} \quad (5)$$

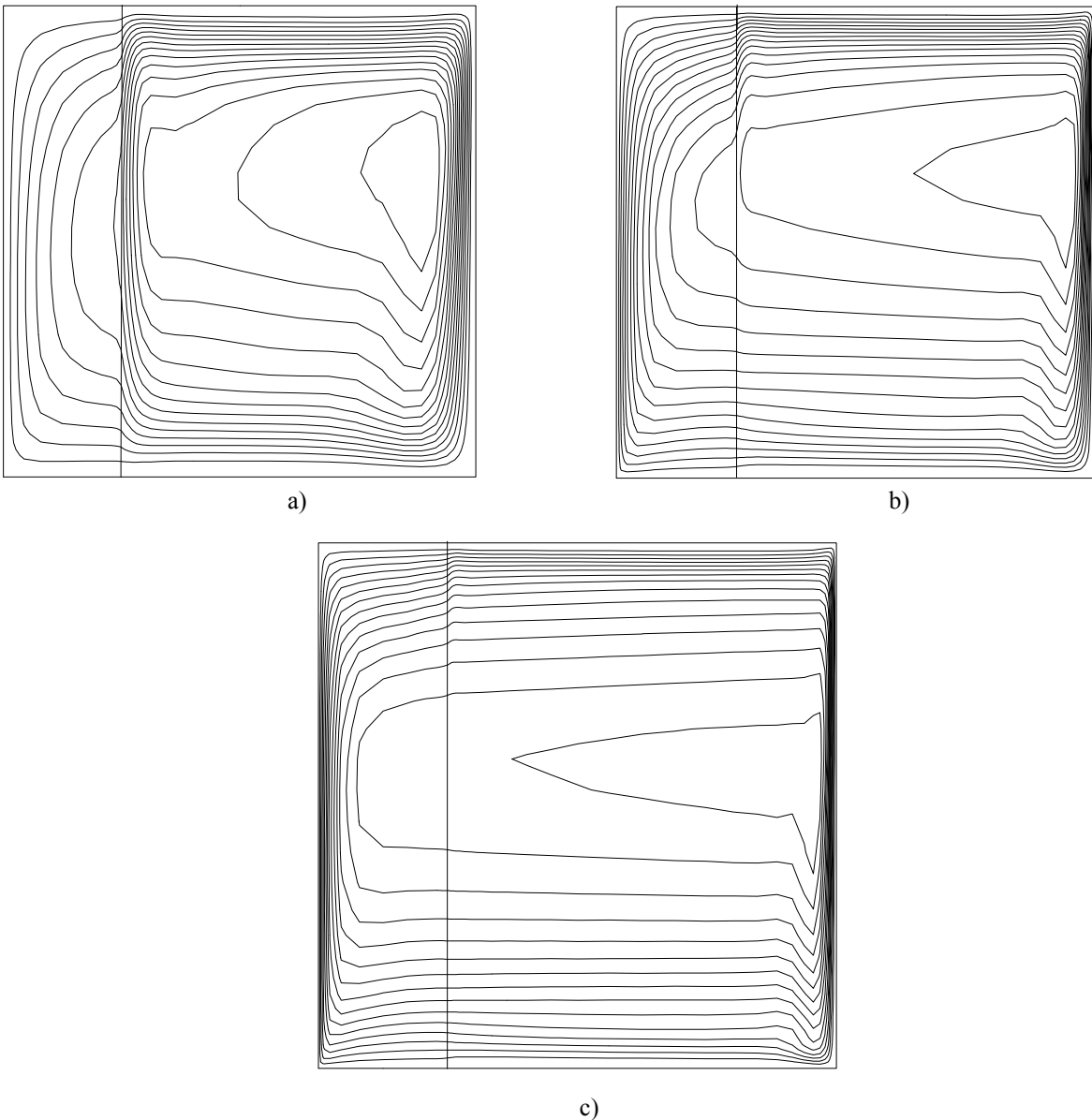


Figure 3 Effect of Rayleigh number on streamlines, $\phi=0.8$, grid 50x50: a) $Ra=10^7$, b) $Ra=10^8$, c) $Ra=10^9$.

Transport equations for $\langle k \rangle^i$ and its dissipation rate $\langle \varepsilon \rangle^i = \mu \overline{\langle \nabla \mathbf{u}' : (\nabla \mathbf{u}')^T \rangle} / \rho$ are proposed in Pedras & de Lemos (2001) as:

$$\rho \left[\frac{\partial}{\partial t} (\phi \langle k \rangle^i) + \nabla \cdot (\bar{\mathbf{u}}_D \langle k \rangle^i) \right] = \nabla \cdot \left[\left(\mu + \frac{\mu_{t_o}}{\sigma_k} \right) \nabla (\phi \langle k \rangle^i) \right] + P^i + G^i + G_\beta^i - \rho \phi \langle \varepsilon \rangle^i \quad (6)$$

$$\rho \left[\frac{\partial}{\partial t} (\phi \langle \varepsilon \rangle^i) + \nabla \cdot (\bar{\mathbf{u}}_D \langle \varepsilon \rangle^i) \right] = \nabla \cdot \left[\left(\mu + \frac{\mu_{t_o}}{\sigma_\varepsilon} \right) \nabla (\phi \langle \varepsilon \rangle^i) \right] + \frac{\langle \varepsilon \rangle^i}{\langle k \rangle^i} [c_1 P^i + c_2 G^i + c_1 c_3 G_\beta^i - c_2 \rho \phi \langle \varepsilon \rangle^i] \quad (7)$$

where c_1, c_2, c_3 and c_k are model constants, $P^i = -\rho \overline{\langle \mathbf{u}' \mathbf{u}' \rangle}^i : \nabla \bar{\mathbf{u}}_D$, $G^i = C_k \rho \frac{\phi \langle k \rangle^i |\bar{\mathbf{u}}_D|}{\sqrt{K}}$ and G_β^i are generation rates of $\langle k \rangle^i$ due to gradients of $\bar{\mathbf{u}}_D$, due to the action of the porous matrix and due to the buoyancy forces in the liquid phase, respectively. A proposal for this last term was made by de Lemos & Braga (2003) and can be written as,

$$G_\beta^i = \phi \frac{\mu_{t_o}}{\sigma_t} \mathbf{g} \beta_\phi \nabla \langle \bar{T} \rangle^i \quad (8)$$

where ν_{t_o} expresses the macroscopic turbulent kinematic viscosity, $\nu_{t_o} = \mu_{t_o} / \rho_f$, β_ϕ is a macroscopic thermal expansion coefficient and σ_T is a constant.

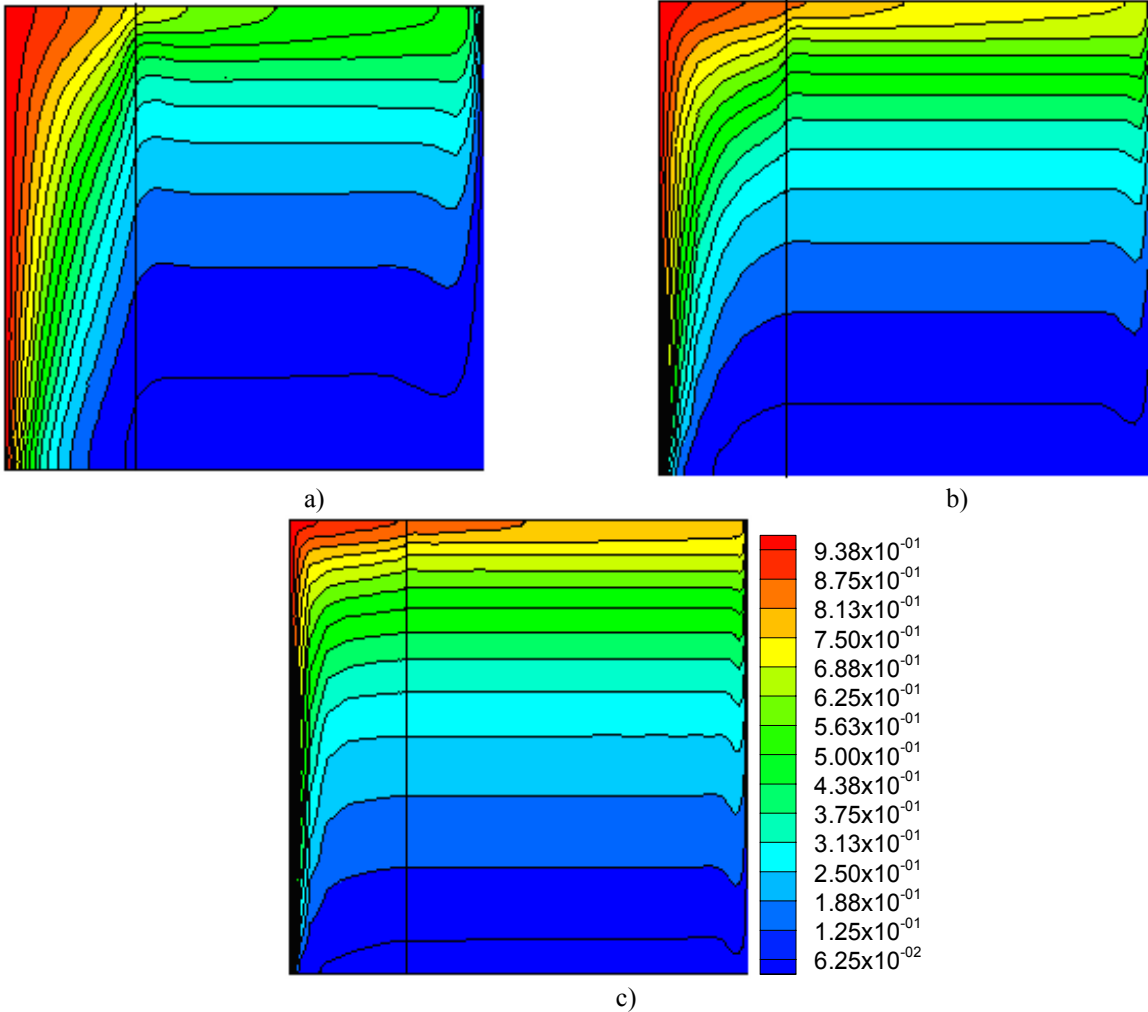


Figure 4 - Effect of Rayleigh number on temperature field, $\phi=0.8$, grid= 50×50 , a) $Ra=10^7$, b) $Ra=10^8$, c) $Ra=10^9$.

2.3 Macroscopic energy equation:

In a similar way, applying both time- and volume-average operators to the microscopic energy equation, for the fluid and for the porous phases, two equations appear. Assuming then the hypothesis of **Local Thermal Equilibrium**, which considers $\langle T_f \rangle^i = \langle T_s \rangle^i = \langle \bar{T} \rangle^i$, and adding up the two obtained equations, one has (see Braga & de Lemos (2002a-e) and de Lemos & Braga (2003) for details),

$$\left\{ (\rho c_p)_f \phi + (\rho c_p)_s (1-\phi) \right\} \frac{\partial \langle \bar{T} \rangle^i}{\partial t} + (\rho c_p)_f \nabla \cdot (\mathbf{u}_D \langle \bar{T} \rangle^i) = \nabla \cdot \left\{ \mathbf{K}_{eff} \cdot \nabla \langle \bar{T} \rangle^i \right\} \quad (9)$$

where

$$\mathbf{K}_{eff} = \left[\phi k_f + (1-\phi) k_s \right] \mathbf{I} + \mathbf{K}_{tor} + \mathbf{K}_t + \mathbf{K}_{disp} + \mathbf{K}_{disp,t} \quad (10)$$

is the effective macroscopic conductivity tensor.

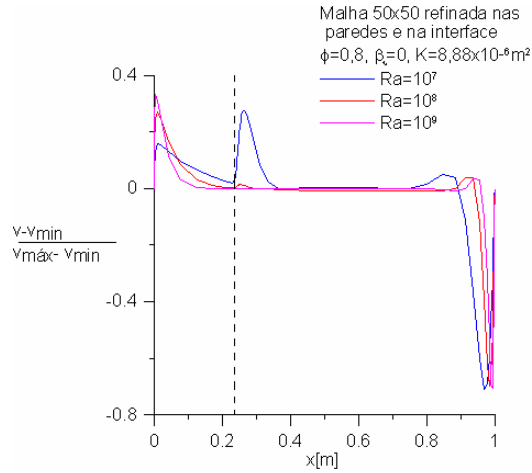


Figure 5 Rayleigh number effect on velocity field, $\phi=0.8$, 50x50 wall and interface refined grid.

At the interface, the conditions of continuity of velocity, pressure, turbulent kinetic energy k and its dissipation rate ε , in addition to their respective diffusive fluxes, are given by,

$$\bar{\mathbf{u}}_D \Big|_{0 < \phi < 1} = \bar{\mathbf{u}}_D \Big|_{\phi=1} \quad (11)$$

$$\langle \bar{p} \rangle^i \Big|_{0 < \phi < 1} = \langle \bar{p} \rangle^i \Big|_{\phi=1} \quad (12)$$

$$\langle k \rangle^v \Big|_{0 < \phi < 1} = \langle k \rangle^v \Big|_{\phi=1} \quad (13)$$

$$\left(\mu + \frac{\mu_{t_\phi}}{\sigma_k} \right) \frac{\partial \langle k \rangle^v}{\partial y} \Big|_{0 < \phi < 1} = \left(\mu + \frac{\mu_t}{\sigma_k} \right) \frac{\partial \langle k \rangle^v}{\partial y} \Big|_{\phi=1} \quad (14)$$

$$\langle \varepsilon \rangle^v \Big|_{0 < \phi < 1} = \langle \varepsilon \rangle^v \Big|_{\phi=1} \quad (15)$$

$$\left(\mu + \frac{\mu_{t\phi}}{\sigma_\varepsilon}\right) \frac{\partial \langle \varepsilon \rangle^v}{\partial y} \Big|_{0 < \phi < 1} = \left(\mu + \frac{\mu_t}{\sigma_\varepsilon}\right) \frac{\partial \langle \varepsilon \rangle^v}{\partial y} \Big|_{\phi=1} \quad (16)$$

The jump condition at the interface is given by,

$$\left(\mu_{ef} + \mu_{t\phi}\right) \frac{\partial \bar{u}_{D_p}}{\partial y} \Big|_{0 < \phi < 1} - \left(\mu + \mu_t\right) \frac{\partial \bar{u}_{D_p}}{\partial y} \Big|_{\phi=1} = \left(\mu + \mu_t\right) \frac{\beta}{\sqrt{K}} \bar{u}_{D_i} \Big|_{\text{interface}} \quad (17)$$

The non-slip condition for velocity is applied to all of the four walls. In this work, the Rayleigh number is calculated with the fluid phase properties and defined as $Ra = g\beta L^3 \Delta T / \nu \alpha$, where g is the gravity acceleration, β is the fluid volumetric expansion coefficient, ν is the fluid kinematic viscosity, α is the thermal diffusivity and $\Delta T = T_H - T_C$.

3. Numerical Method

The equations above were discretized in the computational mesh shown in Figure 2. This mesh concentrates nodal points close to the four walls and around the interface.

The numerical method used in the resolution of the equations above was the Finite Volumes technique and the *SIMPLE* algorithm of Patankar (1980). The interface is positioned to coincide with the border between two control volumes, generating, in such a way, only volumes of the types 'totally porous' or 'totally clear'. The flow and energy equations are resolved then in the porous and clear domains, being respected the interface conditions mentioned earlier.

4. Results and Discussion

The geometry and computational grids used in this work are shown in Figure 1 and Figure 2, respectively. The analysis on this section will focus only on the effect of Rayleigh number on streamlines and on both velocity and temperature fields. Also, here only the cavity having 25% of porous material will be studied (Figure 1b) since case a) in Figure 1 has been the subject of other works [Magro & de Lemos (2002c), de Lemos & Magro (2003)].

Figure 3 shows the effect of Rayleigh number on the hydrodynamic field for both clean and porous media, with 25% porous material. It can be observed that, with the increasing Rayleigh number, the flow penetrates the porous medium more intensively. For $Ra > 10^8$, it becomes clear the existence of a boundary layer both on right face (clear medium) and on the contact surface between of the porous medium and the left wall. For $Ra = 10^9$, despite the center of the recirculation zone is still located within the unobstructed volume, there is a considerable convective flow through the porous matrix. It can be seen that, in this cavity, the flow behaves much like as in the case of a cavity filled with 50% porous material, cases a) in Figure 1 (Magro & de Lemos (2002c), de Lemos & Magro (2003)).

The effect of Rayleigh number on temperature field is presented in Figure 4. It can be seen that the stratification on the temperature field, with the increasing of the Rayleigh number, also begins to appear inside the porous layer. For $Ra = 10^9$, the temperature field shows a nearly fully stratified behavior and a thin boundary layer develops along the lateral walls.

Figure 5 details the development of the observed boundary layer along the lateral surfaces. As already mentioned, with increase in Ra the convective flow penetrates more intensively on the porous substrate, returning down mostly along the right wall. It is interesting to observe a peak at the interface to $Ra = 10^7$, most likely due to the relatively strong resistance to flow within the porous medium at this condition. For higher vales of Ra , however, the fluid processes more momentum being able to enter the porous structure and maintain the most of the flow within the boundary layers along the walls.

The Nusselt number calculated by,

$$\overline{Nu} = \frac{1}{H} \int_0^H Nudy \quad (18)$$

where

$$Nu = \frac{\partial T}{\partial x} \Big|_{x=0} \frac{L}{T_H - T_C} \quad (19)$$

is taken along the wall were the higher temperature T_H prevails. The effect of Ra on the value of Nu is documented in Table 1. For both calculated porosities, there is an increase on Nu as Ra increases, reflecting the enhancement of the

convective currents as Ra attains higher values. For a given Ra , the same effect seems to occur on Nu as the porosity ϕ increases.

Table 1 – Nusselt number for vertical cavity with porous material, grid 50×50.

$\phi \setminus Ra$	10^7	10^8	10^9	10^{10}
Cavity with 50% Porous Material (from Magro & de Lemos (2002c) and de Lemos & Magro (2003))				
Grid refined close to the walls				
0.5	1.69	2.65	9.39	28.72
0.8	4.39	13.18	30.52	67.05
Grid refine on walls and around the interface				
0.8	4.37	13.15	30.46	67.0
Cavity with 25% Porous Material				
Grid refine on walls and around the interface				
0.8	5.164	13.7	30.56	

The comparison between the wall-refined grid and the wall-and-interface-refine grid shows an agreement related to Nusselt number, indicating that for the conditions here analyzed the solution is nearly grid independent. Finally, comparing Nusselt numbers for 50% and 25% porous medium thicknesses, it can be seen that, for $Ra=10^7$, there is an increase on Nusselt number. However, for $Ra=10^9$, only a slight enhancement on Nusselt number is observed, indicating that the higher the Rayleigh number, the less important seems to be the size of the porous material. However, since calculations herein were performed for materials with certain thermal-physical properties, and considering further that the heat across the cavity propagates by the mechanisms of conduction and convection, the tendencies here observed might be not occurs if other values of the fluid and solid properties were employed.

5. Concluding Remarks

In this work, numerical results were presented for laminar and turbulent flows in hybrid domains with heat transfer, which involved an interface between the porous bed and the clear medium. The used numerical method made possible the simultaneous treatment of the porous matrix and of the unobstructed region as a single calculation domain, naturally considering the interface conditions between the two media. The Raleigh number was varied and the change in global heat transfer across the cavity was obtained. It was observed that an increase in Ra intensified convective currents inside of the porous material, leading to the situation of stratification of the temperatures field in the entire domain of calculation. The increment on the heat transferred was also observed with the increase of the porosity of the material.

6. Acknowledgments

The authors would like to thank CNPq, Brazil, for their financial support during the preparation of this work.

7. References

- Antohe, B.V.; Lage, J.L., 1997, "A general two-equation macroscopic turbulence model for incompressible flow in porous media", *Int. J. Heat Mass Transfer*, vol. 40, pp. 3013-3024.
- Braga, E.J., de Lemos, M.J.S., 2002a, FREE CONVECTION IN SQUARE AND RECTANGULAR CAVITIES HEATED FROM BELOW OR ON THE LEFT, *Proc. CONEM2002, 3rd Congresso Nacional de Engenharia Mecânica*, João Pessoa, PB, Brazil, August 12-16.
- Braga, E.J., de Lemos, M.J.S., 2002b, LAMINAR NATURAL CONVECTION IN CONCENTRIC AND ECCENTRIC ANNULI, *Proceedings of ENCIT2002, 9th Brazilian Congress of Thermal Engineering and Sciences* (on CD-ROM), Caxambu, MG, Brazil, October 13-17.
- Braga, E.J., de Lemos, M.J.S., 2002c, NATURAL CONVECTION IN TURBULENT REGIME IN CONCENTRIC AND ECCENTRIC HORIZONTAL ANNULAR REGIONS, **Paper AIAA-2002-3316**, *Proc. of 8th AIAA/ASME, Joint Thermophysics and Heat Transfer Conference*, St Louis, Missouri, U.S.A, June 23-27.
- Braga, E.J., de Lemos, M.J.S., 2002d, NATURAL CONVECTION IN CAVITIES COMPLETELY FILLED WITH POROUS MATERIAL, *Proceedings of APM2002, 1st International Conference on Applications of Porous Media*, **Paper APM-164**, vol. 1, pp. 551-560, Jerba, Tunisia, June 2-8.
- Braga, E.J., de Lemos, M.J.S., 2002e, Turbulent Natural Convection in Enclosures Completely Filled With Porous Material, **Paper IMECE2002-34403**, *2002 ASME International Mechanical Engineering Congress*, New Orleans, LA, USA, November 17-22, 2002.

- Charrier-Mojtabi, M.C., 1997, NUMERICAL SIMULATION OF TWO –AND –THREEDIMENSIONAL FREE CONVECTION FLOWS IN A HORIZONTAL POROUS ANNULUS USING A PRESSURE AND TEMPERATURA FORMULATION, *Int. J. Heat Mass Transfer*, vol, 40(7), pp. 1521-1533.
- de Lemos, M.J.S., Braga, E.J., 2003, MODELING OF TURBULENT NATURAL CONVECTION IN SATURATED RIGID POROUS MEDIA, *Int. Comm. Heat and Mass Transfer*, (accepted).
- de Lemos, M.J.S., Magro, V.T., 2003, Turbulent Free Convection in a Composite Enclosure, accepted for presentation at 2003 ASME Heat Transfer Conference, Las Vegas, NV, USA, July 21-23.
- de Vahl Davis, G., 1983, Natural convection in a square cavity: A benchmark numerical solution, *Int. J. Num. Methods in Fluids*, vol 3, pp. 249-264.
- Magro, V.T., de Lemos, M.J.S., 2002a, “Convecção Natural em Regime Laminar em Cavidade Contendo Material Poroso” (In Portuguese), Proc. CONEM 2002 - II Congresso Nacional de Engenharia Mecânica, João Pessoa, PA, 23-28 Agosto.
- Magro, V.T., de Lemos, M.J.S., 2002b, “Efeito da Permeabilidade e Porosidade na Convecção Natural em Cavidade contendo Material Poroso” (In Portuguese), Proc ENCIT 2002 - Congresso Brasileiro de Engenharia e Ciências Térmicas, Caxambu, MG, Brazil, 15-18 October.
- Magro, V.T., de Lemos, M.J.S., 2002c, “Convecção Natural em Regime Turbulento em Cavidade Contendo Material Poroso”, ETT 2002 - Escola de Transição e Turbulência, Florianópolis, SC, 23 a 27 de Setembro.
- Ochoa-Tapia, J.A.; Whitaker, S., 1995, “Momentum transfer at the boundary between a porous medium and a homogeneous fluid-I. Theoretical development”, *Int. J. Heat Mass Transfer*, vol. 38, pp. 2635-2646.
- Patankar, S.V., 1980, NUMERICAL HEAT TRANSFER AND FLUID FLOW, Mc-Graw Hill.
- Pedras. M.H.J., de Lemos, M.J.S., 2001, Macroscopic Turbulence Modeling For Incompressible Flow Through Undeformable Porous Media, *Int. J. Heat Transfer*, vol. 44(6), pp. 1081-1093.
- Rocamora, F.D.J., de Lemos, M.J.S., 2000, Analysis Of Convective Heat Transfer For Turbulent Flow In Satured Porous Media, *Int. Comm. Heat Mass Transfer*, vol. 27(6), pp. 825-834
- Silva, R.A., de Lemos, M.J.S., 2002, “Numerical Treatment of the Stress Jump Interface Condition for Laminar Flow in a Channel Containing a Porous Layer”, *Numerical Heat Transfer – Part A*, vol. 43(6), pp. 603-617.